Power Spectrum of MSK-Type Modulations in the Presence of Data Imbalance

M. K. Simon,[1] P. Arabshahi,[1] L. Lam,[1] and T.-Y. Yan[1]

Using the amplitude-modulation pulse (AMP) representation of continuous-phase modulation (CPM) introduced more than a decade ago by Laurent, the power spectral density (PSD) of minimum-shift-keying (MSK)-type modulations (modulation index equal to one-half) is computed in the presence of data imbalance. The advantage of this technique is that closed-form expressions can be obtained that clearly elucidate the partitioning of the spectrum into components due to the effective AMP pulse shapes and those due to the AMP sequence correlations. As such, these expressions give insight into the nature of the PSD distortion produced by the imbalance, i.e., a tilt in the main lobe and a relative unbalance between the upper and lower side-lobe levels caused by the correlation between the in-phase (I) and quadrature-phase (Q) components of the complex AMP data sequences and the correlation between the sequences themselves. It is demonstrated that data imbalance does not change the rate *at which the side lobes roll off. It also is shown that, for all practical purposes, the PSD can be computed based on a two-pulse stream AMP approximation.*

I. Introduction

It is well-known that continuous-phase modulation (CPM) is a modulation scheme that in addition to being bandwidth efficient offers the advantage of being constant envelope, the latter being significant in systems employing nonlinear amplification. One class of CPM is the group of so-called minimum-shift-keying (MSK)-type modulations that all have modulation index $h = 0.5$ and are distinguished from one another by the shape of the frequency pulse that modulates the transmitted carrier. MSK itself corresponds to a rectangular frequency pulse of duration equal to a bit time, T_b. The reason this group is of interest is that it lends itself to an in-phase–quadrature-phase (I–Q) form of receiver implementation. The evaluation of the power spectral density (PSD) of conventional (corresponding to a balanced random binary data input) angle and frequency modulations has been described in many places in the literature, e.g., [1–6], and specific results have been documented for a variety of popular full- and partial-response MSK-type schemes, including MSK itself, Gaussian MSK (GMSK), and tamed-frequency modulation (TFM).

In addition to pulse shaping, the presence of data imbalance (unequal probabilities for the $+1$'s and -1's) can have a profound effect on the PSD of digital modulations, so much so that standards committees such as the Consultative Committee for Space Data Systems (CCSDS) have included in their specifications

[1] Communications Systems and Research Section.

a limit on the amount of imbalance that can be tolerated [12]. For linear modulations such as amplitude modulation of a binary pulse stream on a carrier, the effect of data imbalance on the PSD is well documented, e.g., [7, Chapter 2], manifesting itself in the addition of a discrete spectral component to the overall PSD with no effect on the *shape* of the continuous component [7]. For phase (or frequency) modulation, the evaluation of the PSD is considerably more complex, and the effect of data imbalance is quite different in terms of its impact on both the discrete and continuous spectral components of the modulator output. Because of these important differences and their significance in relation to the specification on the tolerable amount of data imbalance, a study of the PSD of MSK-type modulations (including GMSK as a specific case of high interest) in the presence of such imbalance is warranted.

Of the many techniques available for evaluating the power spectral density of CPM schemes [1–4], the one deemed most convenient by the authors, particularly for MSK-type modulations with data imbalance, is that which results from a CPM signal representation introduced more than a decade ago by Laurent [4]. In particular, Laurent described an exact representation for CPM in the form of a superposition of a number of time-/phase-shifted amplitude-modulation pulse (AMP) streams. The number of such streams was dependent on the partial-response nature of the modulation as described by the duration, L (in symbols), of the frequency pulse that characterizes the CPM. For binary pulse streams,[2] the number of pulse streams in the AMP representation is 2^{L-1}. Laurent's primary motivation for presenting such a representation was that it allowed for easy evaluation of the autocorrelation and PSD of such modulations, particularly for half-integer index modulations, i.e., ones whose frequency-modulation index was of the form $h = n + 1/2, n$ integer, which includes the case of interest here (i.e., $n = 0$). Specifically, when the input binary data were random and balanced, the complex data sequences that characterize each of the 2^{L-1} AMP components are themselves uncorrelated and, furthermore, are uncorrelated with each other. As such, the PSD of the composite CPM waveform is equal to the sum of the PSDs of the AMP components, each of which is computed by conventional PSD evaluation techniques for binary amplitude (unit magnitude) modulation of a carrier with a complex independent identically distributed (i.i.d.) data sequence.

In this article, we expand upon the PSD evaluation found in Laurent to include the case of input data imbalance. Specifically, we shall show that, because of the presence of data imbalance, the effective complex data sequences that typify each AMP pulse stream are now themselves correlated and, furthermore, are correlated with each other. The correlation properties of each of these sequences resemble those of a first-order Markov process and, hence, the PSD for each contains a factor due to the pulse shape as well as a factor due to the sequence correlation. Likewise, the cross-correlation properties of the sequences contain pulse shape and correlation factors.

We begin the article by reviewing the Laurent representation for MSK-type modulations. Following this, we present the generic result for the PSD of a modulation composed of a group of correlated data pulse trains each of which contains its own real pulse shape and complex data stream. Next, we apply this generic PSD formula first to MSK and then to GMSK. Since MSK is a full-response scheme, its Laurent representation has only a single pulse stream and, thus, the PSD has no cross-correlation components. Since GMSK can be approximated by a $4T_b$-wide frequency pulse at the output of the Gaussian filter, it is a partial-response scheme with a Laurent representation having $2^{L-1} = 8$ pulse streams. However, Kaleh [9] explicitly showed that, for GMSK with a bandwidth-bit time product $BT_b = 0.25$ and a $4T_b$-wide approximation of the Gaussian pulse, i.e., $L = 4$, a two-pulse-stream approximation is for all practical purposes (the fraction of energy in the neglected six pulse streams is 2.63×10^{-5}) exact. Thus, in evaluating the PSD of GMSK, we shall employ this two-pulse-stream approximation of the Laurent representation.

---

[2] The work later was extended to the M-ary case by Mengali and Morelli [8].

II. Laurent Representation of MSK-Type Modulations

The classical representation of an MSK-type of CPM modulation has the form

$$s(t) = \sqrt{\frac{2E_b}{T_b}} \cos\left(\omega_c t + \phi\left(t, \boldsymbol{\alpha}\right) + \phi_0\right), \quad nT_b \le t \le (n+1)T_b \tag{1}$$

where E_b and T_b, respectively, denote the energy and duration of a bit ($P = E_b/T_b$ is the signal power), $\omega_c = 2\pi f_c$ is the radian carrier frequency, $\boldsymbol{\alpha} = (\cdots, \alpha_{-2}, \alpha_{-1}, \alpha_0, \alpha_1, \alpha_2, \ldots)$ is the i.i.d. binary (± 1) data sequence, $\phi\left(t, \boldsymbol{\alpha}\right)$ is the equivalent phase-modulation process, which is expressible in the form of a digital pulse stream,

$$\phi\left(t, \boldsymbol{\alpha}\right) = \pi \sum_{i \le n} \alpha_i q\left(t - iT_b\right) \tag{2}$$

and $q(t) = \int_{-\infty}^{t} g\left(\tau\right) d\tau$ is the *normalized phase-smoothing response* that defines how the underlying phase, $\pi\alpha_i$, evolves with time. In general, $q(t)$ extends over infinite time and satisfies the following:

$$q(t) = \begin{cases} 0, & t \le 0 \\ \dfrac{1}{2}, & t \ge LT_b \end{cases} \tag{3}$$

In what follows, it will be convenient to deal with the normalized (unit-amplitude) complex envelope of $s(t)$, i.e., the complex baseband signal $\tilde{S}(t)$ defined by the relation

$$\tilde{S}(t) = \exp\left\{j\phi\left(t, \boldsymbol{\alpha}\right)\right\}, \quad nT_b \le t \le (n+1)T_b \tag{4}$$

Define the generalized phase-pulse function by

$$\Psi(t) = \begin{cases} \pi q(t), & 0 \le t \le LT_b \\ \dfrac{\pi}{2}\left[1 - 2q\left(t - LT_b\right)\right], & LT_b \le t \end{cases} \tag{5}$$

which is obtained by taking the nonconstant part of $q(t)$, i.e., the part that exists in the interval $0 \le t \le LT_b$, and reflecting it about the $t = LT_b$ axis. Thus, in view of Eq. (5), $\Psi(t)$ is a waveform that is nonzero in the interval $0 \le t \le 2LT_b$ and symmetric around $t = LT_b$. The importance of $\Psi(t)$ is that it allows definition of the following functions, which become an integral part of the AMP representation of GMSK:

$$S_0(t) = \sin \Psi(t) \tag{6}$$

$$S_n(t) = S_0(t + nT_b) = \sin \Psi(t + nT_b) \tag{7}$$

Next one defines a series of pulse shapes $C_i\left(t\right),\ i = 1, 2, \cdots, 2^{L-1}$, each made up of L-fold distinct products of the $S_n\left(t\right)$'s. For example, for GMSK with $L = 4$, the $2^{L-1} = 8$ distinct pulse shapes are [4, Eq. (11)]

$$\left.\begin{aligned}
C_0(t) &= S_0(t)S_1(t)S_2(t)S_3(t), \quad 0 \le t \le 5T_b \\
C_1(t) &= S_0(t)S_2(t)S_3(t)S_5(t), \quad 0 \le t \le 3T_b \\
C_2(t) &= S_0(t)S_1(t)S_3(t)S_6(t), \quad 0 \le t \le 2T_b \\
C_3(t) &= S_0(t)S_3(t)S_5(t)S_6(t), \quad 0 \le t \le 2T_b \\
C_4(t) &= S_0(t)S_1(t)S_2(t)S_7(t), \quad 0 \le t \le T_b \\
C_5(t) &= S_0(t)S_2(t)S_5(t)S_7(t), \quad 0 \le t \le T_b \\
C_6(t) &= S_0(t)S_1(t)S_6(t)S_7(t), \quad 0 \le t \le T_b \\
C_7(t) &= S_0(t)S_5(t)S_6(t)S_7(t), \quad 0 \le t \le T_b
\end{aligned}\right\} \tag{8}$$

each of which is a product of the basic generalized pulse shape $S_0(t)$ and $L-1=3$ other time shifts of $S_0(t)$. Finally, then the generic AMP form for the complex envelope of MSK-type signals is [4]

$$\tilde{S}(t) = \sum_{K=0}^{2^{L-1}-1} \left[\sum_{n=-\infty}^{\infty} j^{A_{K,n}} C_K\left(t - nT_b\right) \right] \triangleq \sum_{K=0}^{2^{L-1}-1} \left[\sum_{n=-\infty}^{\infty} \tilde{a}_{K,n} C_K\left(t - nT_b\right) \right] \tag{9}$$

which results in the real signal

$$s(t) = \sqrt{\frac{2E_b}{T_b}}\ \mathrm{Re}\left\{\tilde{S}(t)\right\} = \sqrt{\frac{2E_b}{T_b}} \sum_{K=0}^{2^{L-1}-1} \left[\sum_{n=-\infty}^{\infty} C_K\left(t - nT_b\right) \cos\left(\omega_c t + \frac{\pi}{2} A_{K,n}\right) \right] \tag{10}$$

i.e., a superposition of 2^{L-1} amplitude-/phase-modulated pulse streams, some of which contain overlapping pulses. Also in Eq. (10), $\tilde{a}_{K,n} \triangleq j^{A_{K,n}} = e^{j(\pi/2)A_{K,n}}$ is the equivalent complex (unit-amplitude) data symbol for the nth transmitted pulse in the Kth stream whose phase $(\pi/2)\,A_{K,n}$ depends solely on the past information data sequence $\boldsymbol{\alpha}$ in a manner described in [4], namely,

$$A_{K,n} = \sum_{l=-\infty}^{n} \alpha_l - \sum_{i=1}^{L-1} \alpha_{n-i}\beta_{K,i} \tag{11}$$

where $\{\beta_{K,i}\}$ are the L coefficients $(0,1)$ in the binary representation of the integer K $\left(0 \le K \le 2^{L-1}-1\right)$. Since, from Eq. (11), $A_{K,n}$ alternates (with n) between even and odd integer values, then $\tilde{a}_{K,n}$ likewise alternates between being purely real (± 1) and purely imaginary $(\pm j)$ values. Thus, as previously mentioned, for each K, $\{\tilde{a}_{K,n}\}$ is a binary amplitude complex data sequence with unit magnitude.

For MSK modulation $(L=1)$, there is only a single pulse stream with pulse shape and data phase

$$\left.\begin{aligned} C_0(t) = S_0(t) = \sin\frac{\pi t}{2T_b}, \quad 0 \le t \le 2T_b \\ A_{0,n} = \sum_{l=-\infty}^{n} \alpha_l \end{aligned}\right\} \tag{12}$$

Thus, the equivalent data symbol $\{\tilde{a}_{0,n}\}$ satisfies the differential encoding relationship

$$\tilde{a}_{0,n} \triangleq e^{j(\pi/2)A_{0,n}} = j\alpha_n \tilde{a}_{0,n-1} \quad \Rightarrow \quad \tilde{a}_{0,2n} \in \{j, -j\}, \quad \tilde{a}_{0,2n+1} \in \{1, -1\} \tag{13}$$

For GMSK, the dominant term is the pulse stream corresponding to $C_0(t)$ since its duration is the longest (at least $2T_b$ longer than any other pulse component) and it also conveys the most significant part of the total energy of the signal. The next most significant term would be the pulse stream corresponding to $C_1(t)$, which contains virtually all the remaining signal energy. Thus, as previously alluded to, it is sufficient to consider only the first two pulse streams in Eq. (9) and, hence, for all practical purposes, we may "exactly" describe GMSK by the complex signal

$$\tilde{S}(t) = \sum_{n=-\infty}^{\infty} \tilde{a}_{0,n} C_0(t - nT_b) + \sum_{n=-\infty}^{\infty} \tilde{a}_{1,n} C_1(t - nT_b) \tag{14}$$

where it can be shown that the equivalent complex data symbols satisfy the relations [9][3]

$$\left.\begin{aligned} \tilde{a}_{0,n} \triangleq e^{j(\pi/2)A_{0,n}} = j\alpha_n \tilde{a}_{0,n-1} \quad \Rightarrow \quad \tilde{a}_{0,2n} \in \{j, -j\}, \quad \tilde{a}_{0,2n+1} \in \{1, -1\} \\ \tilde{a}_{1,n} \triangleq e^{j(\pi/2)A_{1,n}} = j\alpha_n \tilde{a}_{0,n-2} \quad \Rightarrow \quad \tilde{a}_{1,2n} \in \{1, -1\}, \quad \tilde{a}_{1,2n+1} \in \{j, -j\} \end{aligned}\right\} \tag{15}$$

Thus, in terms of the real GMSK signal $s(t)$, we can view it as being composed of the sum of two pulse-shaped offset QPSK-type signals with pulse shapes corresponding to $C_0(t)$ and $C_1(t)$ and I, Q ± 1 data-symbol ($T_s = 2T_b$ in duration) sequences, respectively, corresponding to

$$\left.\begin{aligned} a_{0,2n} = \mathrm{Im}\{\tilde{a}_{0,2n}\}, \quad b_{0,2n+1} = \mathrm{Re}\{\tilde{a}_{0,2n+1}\} \\ a_{1,2n} = \mathrm{Re}\{\tilde{a}_{1,2n}\}, \quad b_{1,2n+1} = \mathrm{Im}\{\tilde{a}_{1,2n+1}\} \end{aligned}\right\} \tag{16}$$

That is,

$$\begin{aligned} s(t) = \sqrt{\frac{2E_b}{T_b}} \Bigg[& \sum_{n=-\infty}^{\infty} a_{0,2n+1} C_0(t - (2n+1)T_b) \cos\omega_c t - \sum_{n=-\infty}^{\infty} b_{0,2n} C_0(t - 2nT_b) \sin\omega_c t \\ & + \sum_{n=-\infty}^{\infty} a_{1,2n} C_1(t - 2nT_b) \cos\omega_c t - \sum_{n=-\infty}^{\infty} b_{1,2n+1} C_1(t - (2n+1)T_b) \sin\omega_c t \Bigg] \end{aligned} \tag{17}$$

[3] Note that the sequence properties of the first sequence in Eq. (15) are identical to those of MSK.

For random i.i.d. balanced input data, $\boldsymbol{\alpha}$, Kaleh [9] shows that the effective data sequences for the two symbol streams as defined in Eq. (16) each has uncorrelated symbols and, furthermore, the two sequences are uncorrelated with each other. As we shall see in a later section, when the data are random i.i.d. but unbalanced, these uncorrelated properties no longer hold.

III. A Generic Expression for the PSD of a Sum of Random Pulse Trains With Complex Data Symbols

Consider finding the PSD of a complex signal $\tilde{S}(t)$ of the form in Eq. (9). The traditional method of evaluating such a PSD is first to find the autocorrelation function of $\tilde{S}(t)$, namely, $R_{\tilde{S}}(t, t+\tau) = E\left\{\tilde{S}(t)\,\tilde{S}^*(t+\tau)\right\}$, then to time average to remove the cyclostationary property, and finally to take the Fourier transform of the result, i.e.,

$$S_{\tilde{S}}(f) = \mathcal{F}\left\{\langle R_{\tilde{S}}(t, t+\tau)\rangle\right\} \tag{18}$$

By a straightforward extension of the results in [7, Chapter 2], the following result can be obtained:

$$S_{\tilde{S}}(f) = \sum_{i=0}^{2^{L-1}-1} S_{ii}(f) + \sum_{i=0}^{2^{L-1}-1}\sum_{\substack{j=0 \\ i<j}}^{2^{L-1}-1} S_{ji}(f) \tag{19}$$

where

$$S_{ii}(f) = S_{\tilde{a}_i}(f)\, S_{p_i}(f) \tag{20}$$

with

$$\left.\begin{aligned} S_{\tilde{a}_i}(f) &= \sum_{l=-\infty}^{\infty} R_{\tilde{a}_i}(l)\, e^{-j2\pi f l T_b}, \quad R_{\tilde{a}_i}(l) = E\left\{\tilde{a}_{i,k}\tilde{a}^*_{i,k+l}\right\} \\ S_{p_i}(f) &= \frac{1}{T_b}\left|P_i(f)\right|^2, \qquad\qquad P_i(f) \triangleq \mathcal{F}\left\{C_i(t)\right\} \end{aligned}\right\} \tag{21}$$

and

$$S_{ji}(f) = 2\ \mathrm{Re}\left\{S_{\tilde{a}_{ji}}(f)\, S_{p_{ji}}(f)\right\} \tag{22}$$

with

$$\left.\begin{aligned} S_{\tilde{a}_{ji}}(f) &= \sum_{l=-\infty}^{\infty} R_{\tilde{a}_{ji}}(l)\, e^{-j2\pi f l T_b}, \quad R_{\tilde{a}_{ji}}(l) = E\left\{\tilde{a}_{j,k}\tilde{a}^*_{i,k+l}\right\} \\ S_{p_{ji}}(f) &= \frac{1}{T_b}P_i(f)\, P_j^*(f), \qquad P_i(f) \triangleq \mathcal{F}\left\{C_i(t)\right\} \end{aligned}\right\} \tag{23}$$

Clearly then, the evaluation of the PSD involves finding the Fourier transform of the various pulse shapes in the AMP representation and both the autocorrelation and cross-correlation of the equivalent complex data sequences.

IV. Cross-Correlation Properties of the Equivalent Complex Data Symbols and Evaluation of the PSD

A. MSK Modulation

For MSK, the equivalent complex data symbols $\{\tilde{a}_{0,n}\}$ are defined in terms of the actual input data symbols $\{\alpha_n\}$ by the iterative relation in Eq. (13). Suppose that $\{\alpha_n\}$ characterizes a random i.i.d. unbalanced source, where

$$\left.\begin{aligned} \Pr\{\alpha_n = 1\} &= 1-p \\ \Pr\{\alpha_n = -1\} &= p \end{aligned}\right\} \tag{24}$$

with $0 \le p \le 1$. Then, it is straightforward to show that $\{\tilde{a}_{0,n}\}$ is a first-order Markov source, and as such, it is balanced, i.e.,

$$\left.\begin{aligned} \Pr\{\tilde{a}_{0,n} = j\} = \frac{1}{2}, \quad \Pr\{\tilde{a}_{0,n} = -j\} = \frac{1}{2} \quad &\text{for } n \text{ even} \\ \Pr\{\tilde{a}_{0,n} = 1\} = \frac{1}{2}, \quad \Pr\{\tilde{a}_{0,n} = -1\} = \frac{1}{2} \quad &\text{for } n \text{ odd} \end{aligned}\right\} \tag{25}$$

and thus $E\{\tilde{a}_{0,n}\} = 0$. However, while the differential encoding operation converts the unbalanced random i.i.d. source to a balanced source,[4] the symbols of the latter are now correlated. Using the defining relation for $\{\tilde{a}_{0,n}\}$, it is straightforward to show that

$$R_{\tilde{a}_0}(l) \triangleq E\left\{\tilde{a}_{0,n}\tilde{a}^*_{0,n+l}\right\} = [-j(1-2p)]^l, \quad l \text{ integer}, \qquad R_{\tilde{a}_0}(-l) = R^*_{\tilde{a}_0}(l) \tag{26}$$

i.e., $\{\tilde{a}_{0,n}\}$ behaves analogously to a first-order Markov source with transition probability equal to p. The discrete Fourier transform of Eq. (26) as needed in Eq. (21) is obtained as

$$S_{\tilde{a}_0}(f) = \sum_{l=-\infty}^{\infty} R_{\tilde{a}_0}(l)\, e^{-j2\pi f l T_b} = \sum_{l=-\infty}^{\infty} [-j(1-2p)]^l\, e^{-j2\pi f l T_b}$$

$$= 1 + 2\sum_{l=-\infty}^{\infty} (1-2p)^l\, e^{-j2\pi l(fT_b+1/4)} \tag{27}$$

Using a well-known result [10] for the series in Eq. (27), namely,

$$\sum_{k=1}^{\infty} a^k \cos k\theta = \frac{a\cos\theta - a^2}{1 - 2a\cos\theta + a^2} \tag{28}$$

[4] The implication of a balanced equivalent complex symbol stream for AMP representation of MSK is that no discrete spectrum will be generated.

we obtain the closed-form result

$$S_{\tilde{a}_0}(f) = \frac{4p(1-p)}{2(1-2p)(1+\sin 2\pi f T_b) + 4p^2} \tag{29}$$

Finally, taking the Fourier transform of the pulse shape in Eq. (12) and substituting its squared magnitude in Eq. (21), the complex baseband PSD of MSK with unbalanced data input becomes

$$S_{\tilde{m}}(f;p) = T_b \frac{16}{\pi^2} \frac{\cos^2 2\pi f T_b}{\left(1 - 16 f^2 T_b^2\right)^2} \left[\frac{4p(1-p)}{2(1-2p)(1+\sin 2\pi f T_b) + 4p^2}\right] \tag{30}$$

Note that because of the presence of the term $\sin 2\pi f T_b$ in the denominator of Eq. (29), the equivalent baseband spectrum of Eq. (30) is not symmetric around $f = 0$. Since the PSD of the true MSK signal as described by Eq. (1) is related to the equivalent baseband PSD by

$$S_s(f;p) = \frac{1}{4}\left[S_{\tilde{m}}(f + f_c;p) + S_{\tilde{m}}(-f + f_c;p)\right] \tag{31}$$

then, equivalently, the PSD of Eq. (31) will have a tilt around the carrier. And since, also from Eq. (30), we have

$$S_{\tilde{m}}(f;1-p) = S_{\tilde{m}}(-f;p) \tag{32}$$

then the tilt of the PSD of Eq. (31) reverses when the probability distribution of the input data is reversed.

Finally, for $p = 1/2$, i.e., balanced random data input, the factor in brackets in Eq. (30) becomes equal to unity, and one obtains the well-known PSD of conventional MSK, namely,

$$S_{MSK}(f) = T_b \frac{16}{\pi^2} \frac{\cos^2 2\pi f T_b}{\left(1 - 16 f^2 T_b^2\right)^2} \tag{33}$$

which is symmetrical around the origin.

B. GMSK Modulation

For GMSK, the equivalent complex data symbols $\{\tilde{a}_{0,n}\}$ are defined in terms of the actual input data symbols $\{\alpha_n\}$ by the iterative relations in Eq. (15). Suppose that $\{\alpha_n\}$ again characterizes a random i.i.d. unbalanced source as described by Eq. (24); then the autocorrelation function of the first equivalent symbol stream is given by Eq. (26) and its associated discrete Fourier transform by Eq. (29). Thus, the PSD of the first component of the AMP representation of GMSK is

$$S_{00}(f;p) = \frac{1}{T_b}\left|P_0(f)\right|^2 \left[\frac{4p(1-p)}{2(1-2p)(1+\sin 2\pi f T_b) + 4p^2}\right], \quad P_0(f) \triangleq \mathcal{F}\{C_0(t)\} \tag{34}$$

with $C_0(t)$ defined in Eq. (8) and evaluated from Eqs. (5), (6), and (7) using for the phase pulse shape

$$q\left(t+\frac{LT_b}{2}\right)=\frac{1}{2}+\frac{1}{2T}\left[\left(t-\frac{T_b}{2}\right)Q\left(\frac{2\pi B}{\sqrt{\ln 2}}\left(t-\frac{T_b}{2}\right)\right)-\left(t+\frac{T_b}{2}\right)Q\left(\frac{2\pi B}{\sqrt{\ln 2}}\left(t+\frac{T_b}{2}\right)\right)\right]$$

$$-\frac{1}{\sqrt{2\pi}}\left(\frac{\sqrt{\ln 2}}{2\pi B}\right)\left[\exp\left\{-\frac{1}{2}\left[\frac{2\pi B}{\sqrt{\ln 2}}\left(t-\frac{T_b}{2}\right)\right]^2\right\}-\exp\left\{-\frac{1}{2}\left[\frac{2\pi B}{\sqrt{\ln 2}}\left(t+\frac{T_b}{2}\right)\right]^2\right\}\right],$$

$$0\le t\le LT_b \quad (35)$$

As mentioned in the introduction, the case of interest here is where $BT_b=0.25$ and $L=4$ so that a two-pulse-stream approximation is sufficient.

Following a procedure similar to that used to derive Eq. (26), it can be shown that the autocorrelation function of the second equivalent symbol stream (which is also balanced and, therefore, has zero mean) is given by

$$R_{\tilde{a}_1}(l)\triangleq E\left\{\tilde{a}_{1,n}\tilde{a}^*_{1,n+l}\right\}=\begin{cases}1, & l=0\\ -j(1-2p)^3, & l=1\\ \left[-j(1-2p)\right]^l, & l\ge 2\end{cases}\quad R_{\tilde{a}_1}(-l)=R^*_{\tilde{a}_1}(l) \quad (36)$$

with discrete Fourier transform

$$S_{\tilde{a}_1}(f)=\sum_{l=-\infty}^{\infty}R_{\tilde{a}_1}(l)\,e^{-j2\pi flT_b}=S_{\tilde{a}_0}(f)+8p(1-2p)(1-p)\sin 2\pi fT_b \quad (37)$$

Thus, the PSD of the second component of the AMP representation of GMSK is

$$\left.\begin{aligned}S_{11}(f;p)&=\frac{1}{T_b}\left|P_1(f)\right|^2 4p(1-p)\left[\frac{1}{2(1-2p)(1+\sin 2\pi fT_b)+4p^2}-2(1-2p)\sin 2\pi fT_b\right]\\ P_1(f)&\triangleq\mathcal{F}\left\{C_1(t)\right\}\end{aligned}\right\} \quad (38)$$

Note again that, because of the presence of the term $\sin 2\pi fT_b$ in the denominator of Eq. (38), the equivalent baseband spectrum is not symmetric around $f=0$.

What remains is to compute the cross-correlation function of the two equivalent complex symbol streams. Following the same procedure as that for obtaining the autocorrelation function of the individual pulse streams, we obtain

$$R_{\tilde{a}_{10}}(l)\triangleq E\left\{\tilde{a}_{1,n}\tilde{a}^*_{0,n+l}\right\}=\begin{cases}\left[-j(1-2p)\right]^{l+1}, & l\ge 0\\ (1-2p)^2, & l=-1\\ \left[j(1-2p)\right]^{-(l+1)}, & l\le -2\end{cases}\quad R_{\tilde{a}_{01}}(-l)=R^*_{\tilde{a}_{10}}(l) \quad (39)$$

with discrete Fourier transform

$$S_{\tilde{a}_{10}}(f)=\sum_{l=-\infty}^{\infty}R_{\tilde{a}_{10}}(l)\,e^{-j2\pi flT_b}=e^{j2\pi fT_b}\left[S_{\tilde{a}_0}(f)-4p(1-p)\right] \quad (40)$$

Thus, the cross-spectrum of $\tilde{m}(t)$is, from Eq. (22),

$$S_{10}(f;p) = 8p(1-p)\ \mathrm{Re}\left\{\left[\frac{1}{2(1-2p)(1+\sin 2\pi f T_b)+4p^2}-1\right]e^{j2\pi f T_b}\frac{1}{T_b}P_0(f)P_1^*(f)\right\} \tag{41}$$

which is also not symmetric around $f = 0$. Finally, the complex baseband PSD of GMSK (based on the two-pulse-stream AMP approximation) with unbalanced data input becomes

$$S_{\tilde{m}}(f;p) = S_{00}(f;p) + S_{11}(f;p) + S_{10}(f;p) \tag{42}$$

where $S_{00}(f;p), S_{11}(f;p)$ and $S_{10}(f;p)$ are defined in Eq. (34) and Eqs. (38) and (41), respectively.

C. Other Pulse Shapes (Raised-Cosine Modulation)

As previously implied, one of the nice features about using the Laurent AMP representation of MSK-type CPM to evaluate its PSD is that this representation clearly allows for isolation of the spectral factor due to pulse shaping and of that due to data-symbol correlation. In fact, the results of Section IV.B are really quite general in that they apply to any partial-response modulation with $L = 4$ if one does not restrict oneself to the phase pulse shape of Eq. (35). In fact, the restriction on the duration of the frequency pulse, i.e., the value of L, also is not an issue. The reason behind this already was intimated when we pointed out the fact that the first AMP equivalent data-symbol sequence for GMSK had identical correlation properties to the single-data-symbol sequence that represents MSK. In a more general context, the following statements can be made about the correlation properties of the equivalent data-symbol sequences in the AMP representation.

Consider two CPM modulation schemes with different amounts of partial response, i.e., one is characterized by a frequency pulse of duration L_1T_b and the other by a frequency pulse of duration L_2T_b (assume $L_2 > L_1$ for convenience). Note that the CPM schemes need not have the same frequency pulse *shape*. Then, from the construction procedure used to derive the equivalent data-symbol sequences of the AMP representation from the true input-data sequence, it is straightforward to show that the first 2^{L_1-1} of the 2^{L_2-1} sequences that represent the second modulation have properties identical to those of the 2^{L_1-1} that completely represent the first modulation. This nicety allows one to consider, for example, a particular class of MSK-type modulations, all having the same frequency-pulse shape but different durations (i.e., different amounts of partial response) and, assuming that a small subset of the total number of AMP pulse streams is sufficient to characterize the PSD, to have to compute the spectral shaping due to the sequence correlation only one time.

A popular class of MSK-type CPM modulations is that corresponding to a raised-cosine (RC) frequency pulse. For this class (originally referred to as sinusoidal-frequency-shift keying (SFSK) by Amoroso [11]), the frequency pulse is given by

$$g(t) = \begin{cases} \dfrac{1}{2LT_b}\left[1-\cos\left(\dfrac{2\pi t}{LT_b}\right)\right], & 0 \le t \le LT_b \\ 0, & \text{otherwise} \end{cases} \tag{43}$$

and for $L = 1$ has a spectral roll-off that varies as f^{-6} (as opposed to an f^{-4} spectral roll-off for MSK). Assuming a two-AMP pulse representation, the PSD for this class (L as a parameter) of modulations would be approximately given by the combination of Eqs. (34), (38), (41), and (42) for $L \ge 2$ or exactly by Eq. (34) for $L = 1$.

Before proceeding with numerical results, we point out that, with some additional computation (which would be warranted if one were interested in very low PSD levels), the PSD evaluation procedure discussed above can be extended to include more than just the first two (dominant) AMP pulse streams. In fact, the results of Section III are quite general and, analogous to Eqs. (26), (36), and (39), all one needs to compute are the autocorrelation and cross-correlation functions of the remainder of the equivalent data symbol streams. For $L = 4$, these remaining six pulse streams are characterized by [9]

$$\left.\begin{aligned}
\tilde{a}_{2,n} &\triangleq (j\alpha_{n-1})\,(j\alpha_n)\,\tilde{a}_{0,n-3} \\
\tilde{a}_{3,n} &\triangleq j\alpha_n \tilde{a}_{0,n-3} \\
\tilde{a}_{4,n} &\triangleq (j\alpha_{n-2})\,(j\alpha_{n-1})\,(j\alpha_n)\,\tilde{a}_{0,n-4} \\
\tilde{a}_{5,n} &\triangleq (j\alpha_{n-2})\,(j\alpha_n)\,\tilde{a}_{0,n-4} \\
\tilde{a}_{6,n} &\triangleq (j\alpha_{n-1})\,(j\alpha_n)\,\tilde{a}_{0,n-4} \\
\tilde{a}_{7,n} &\triangleq j\alpha_n \tilde{a}_{0,n-4}
\end{aligned}\right\} \tag{44}$$

V. Precoded MSK-Type Modulations

Conventional I–Q-type receivers for MSK-type modulations suffer a small performance penalty due to the inherent differential encoding operation (see, for example, Eq. (13) for MSK itself) performed at the transmitter and the attendant requirement for differential decoding at the receiver. A simple fix to this problem is to *precode* the input data with a *differential decoder* [7, Chapter 10], which in effect cancels the differential encoding operation at the transmitter and eliminates the need for differential decoding at the receiver. From a spectral standpoint, this precoding operation has no effect on the PSD of the transmitted signal when the input data are balanced. However, when the input data are unbalanced, as in the case of interest in this article, the precoder has a definite effect on the transmitted signal PSD. To see how this comes about, we first shall consider the simple case of MSK itself.

Suppose that prior to phase modulation of the carrier the input data stream $\boldsymbol{\alpha} = (\cdots, \alpha_{-2}, \alpha_{-1}, \alpha_0, \alpha_1, \alpha_2, \cdots)$ first is converted to a complex data stream via

$$\alpha'_n = \alpha_n j^n \tag{45}$$

and then passed through a differential decoder that satisfies the recursion relation

$$\beta_n = -j\alpha'_n \left(\alpha'_{n-1}\right)^* \tag{46}$$

where β_n denotes the complex binary output of the decoder (input to the MSK modulator) in the nth bit interval. Substituting Eq. (45) into Eq. (46), we see that

$$\beta_n = -j\,(\alpha_n j^n)\left(\alpha_{n-1}\,(-j)^{n-1}\right) = \alpha_n \alpha_{n-1} \tag{47}$$

which is a conventional differential decoding of the true input data bits. Since the cascade of the differential encoder of Eq. (13) and the differential decoder of Eq. (46) produces a unity gain transmission path, i.e.,

$$\beta_n = -j\tilde{a}_{0,n}\tilde{a}^*_{0,n-1} = -j\left(j\alpha_n\tilde{a}_{0,n-1}\right)\tilde{a}^*_{0,n-1} = \alpha_n\left|\tilde{a}_{0,n-1}\right|^2 = \alpha_n \tag{48}$$

then one can deduce that, for an input binary complex i.i.d. bit sequence $\boldsymbol{\alpha}' = (\ldots, \alpha'_{-2}, \alpha'_{-1}, \alpha'_0, \alpha'_1, \alpha'_2, \ldots)$ as in Eq. (45), precoded MSK using the precoder (differential decoder) in Eq. (46) is exactly the same as a Laurent representation of MSK [a single complex symbol-pulse stream with half-sinusoidal pulse shape as in Eq. (13)] with the same input data sequence, i.e., $\{\tilde{a}_{0,n}\} = \boldsymbol{\alpha}'$. This equivalence is illustrated in Fig. 1.

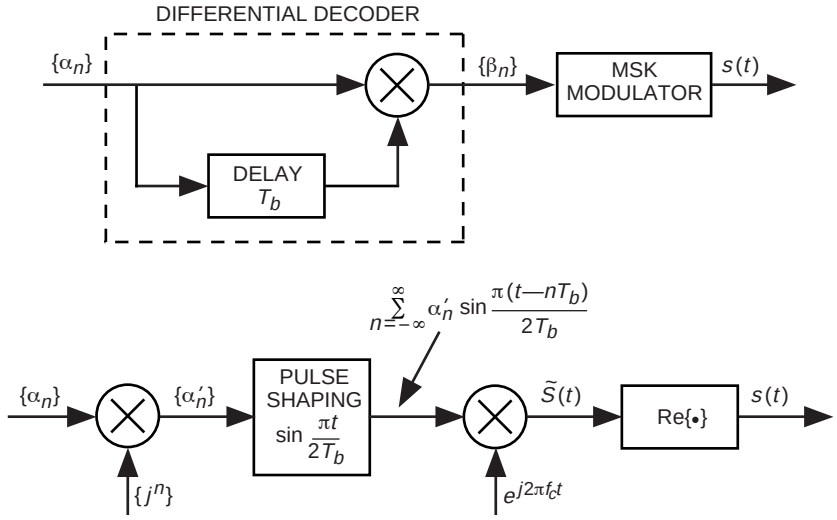

Fig. 1. Equivalent real forms of precoded MSK transmitters.

The upshot of the above equivalence is that, since the conversion from $\boldsymbol{\alpha}$ to $\boldsymbol{\alpha}'$ does not change the statistical (correlation) properties of the sequence, then, based on the Laurent AMP representation, we conclude that the PSD of precoded MSK is that of a linear modulation with an i.i.d. *uncorrelated* complex unbalanced data source and, as such, has a continuous component given by [see Eq. (33)]

$$S_{P-MSK}(f)\,|_{cont} = 4p(1-p)T_b\frac{16}{\pi^2}\frac{\cos^2 2\pi f T_b}{\left(1-16f^2T_b^2\right)^2} \tag{49}$$

and a discrete component derived analogously to [9, Chapter 2] as

$$S_{P-MSK}(f)\,|_{discr} = (1-2p)^2\sum_{k=-\infty}^{\infty}\frac{4}{\pi^2}\frac{1}{\left(1-4k^2\right)^2}\delta\left(f-\frac{k}{2T_b}\right) \tag{50}$$

where $P-MSK$ denotes precoded MSK. Thus, in summary, the addition of a precoder to the input of an MSK modulator with unbalanced data input removes the tilt of the MSK spectrum due to the unbalance and replaces it with a discrete spectral component as is typical of linear modulations.

For GMSK, since each AMP data stream has its own form of "differential encoding" in terms of the relation between its equivalent symbols and the input bits, any precoder that would be used prior

to the GMSK modulator would not compensate all of the data streams. However, since, as previously mentioned, the first data stream [whose equivalent data symbols are a true complex differential encoding of the input bits as per the first of the two equations in Eq. (15)] is the dominant contributor to the overall representation, it seems fortuitous to employ the same precoder as that used for MSK. When this is done, the first data stream in the AMP representation will now have uncorrelated complex symbols, but the second (and, for that matter, the other six) components still will have correlated symbols. However, because of the dominance of the first pulse stream over the others, one would anticipate, analogously to the MSK behavior described above, the presence of a discrete component in the spectrum and a major reduction in the tilt of the continuous component due to the input data unbalance.

VI. Numerical Evaluations and Simulation Results

Using MATLAB software to evaluate the analytical results, Figs. 2(a) and 2(b) illustrate the complex baseband PSD of unbalanced MSK [see Eq. (30)] for $p = 0.45$ (10 percent unbalance), a typical value

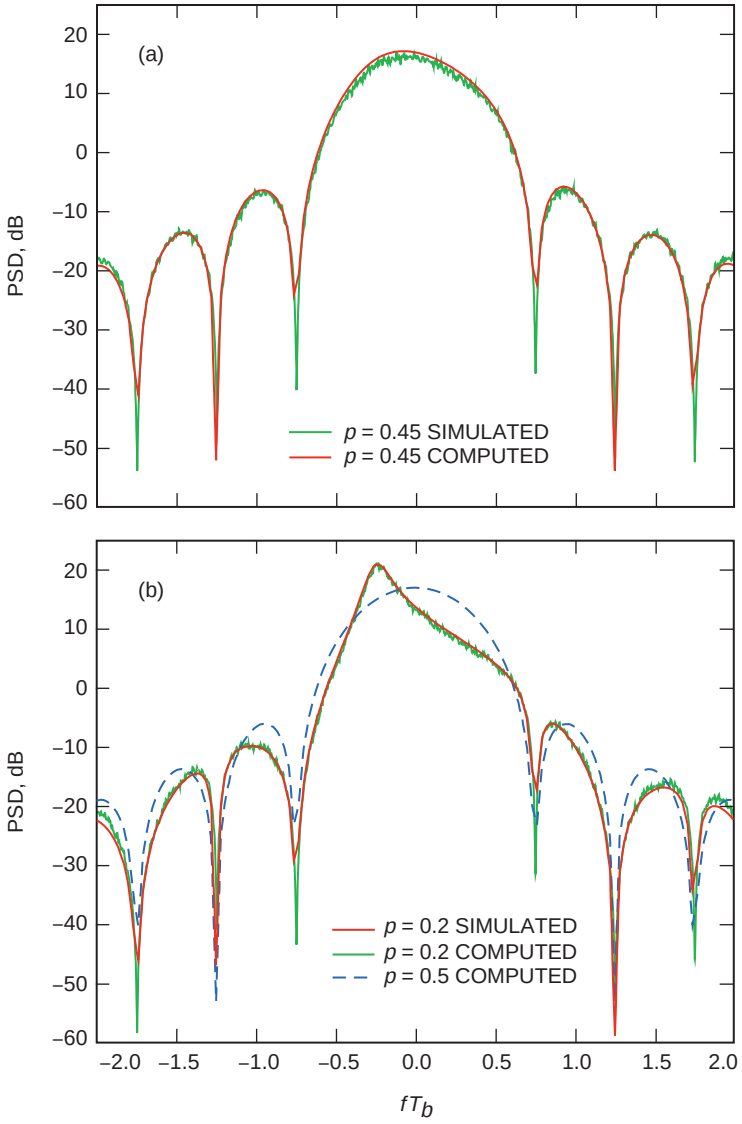

Fig. 2. The complex baseband power spectral density of unbalanced MSK: (a) $p = 0.45$ and (b) $p = 0.2$.

of a standard specification [12], and $p = 0.20$ (60 percent unbalance), which clearly is an extreme case. The PSD for the conventional balanced-data ($p = 0.5$) MSK case [see Eq. (33)] is included for comparison in the latter of the two figures. Superimposed on the calculated PSD curves are numerical results (jagged curve) obtained from a computer simulation of the true GMSK spectrum, which is tantamount to considering all eight AMP components. The GMSK transmitter was simulated using the Signal Processing Worksystems (SPW) software from Cadence Design Systems Inc. and is illustrated in block diagram form in Fig. 3. Evaluation of the simulated PSDs involves two steps. First, 100 blocks of data, each with 256 symbols, were formed, and a Bartlett window was applied to each block. The Bartlett window was chosen because of its low noise floor and the fact that it contributes negligible distortion to the evaluation of the PSDs. Second, a fast Fourier transform (FFT) was performed on each windowed block, and all 100 FFTs were summed and normalized to produce the final PSD result.

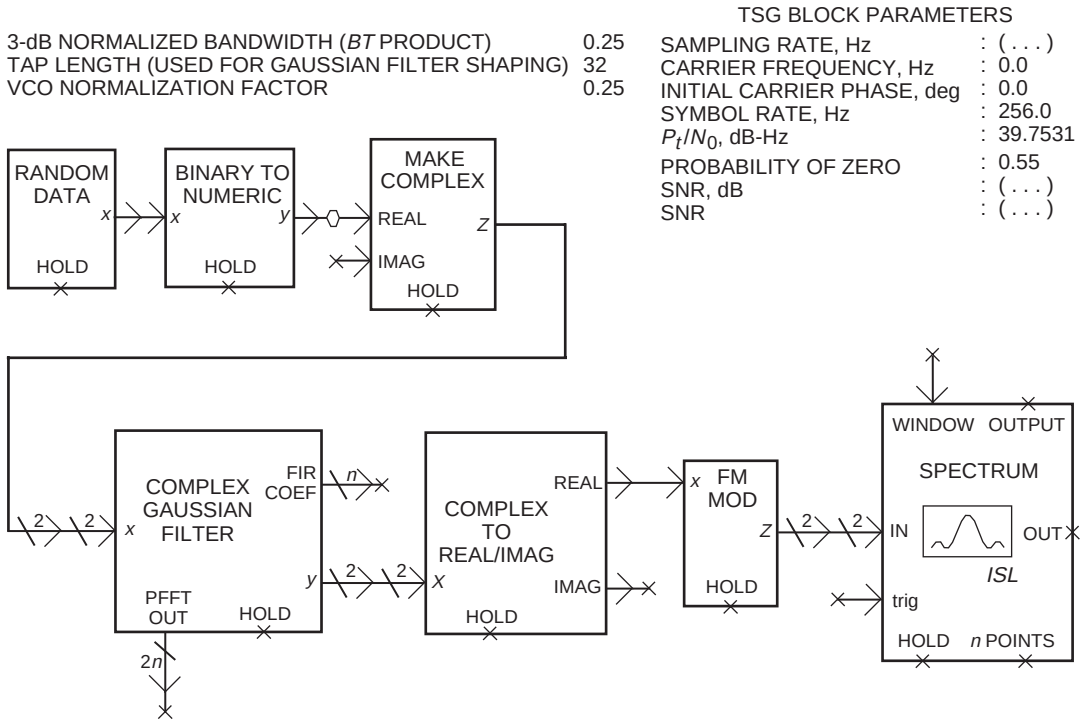

Fig. 3. Computer simulation block diagram of the GMSK transmitter.

We observe from the results in Figs. 2(a) and 2(b) that the asymmetry is such as to increase the side lobes on one side of the spectrum center and decrease them on the other. However, the *rate* at which the side lobes roll off apparently is not changed by the unbalance in the data. The primary effect of the data unbalance on the PSD is to cause a tilt in its main lobe. Also, for the complementary values $p = 0.55$ and $p = 0.80$, the illustrations in Fig. 2(a) and 2(b) simply would be reversed with respect to the frequency axis, i.e., the tilt flips with respect to $f = 0$. Finally, the PSD for the real MSK bandpass waveform would tilt in one direction around $f = f_c$ and in the exact opposite direction around $f = -f_c$. The tilt for the upper side band around $f = f_c$ would be the reverse of that for the complex baseband spectrum because of the reversal of the frequency axis in the relation between these two spectra, as per Eq. (31).

Before showing the PSD of unbalanced GMSK, we first attempt to justify the assumption of using only the first two terms in the Laurent AMP representation to model the transmitted signal. Figure 4 illustrates the PSD of GMSK for $L = 4$ and $BT_b = 0.25$ computed from all $2^{L-1} = 8$ AMP components as well as from only the first two components. As can be seen from the results, the two are virtually identical down to a level of about -70 dB. Thus, we suspect that, for unbalanced GMSK, one can anticipate a

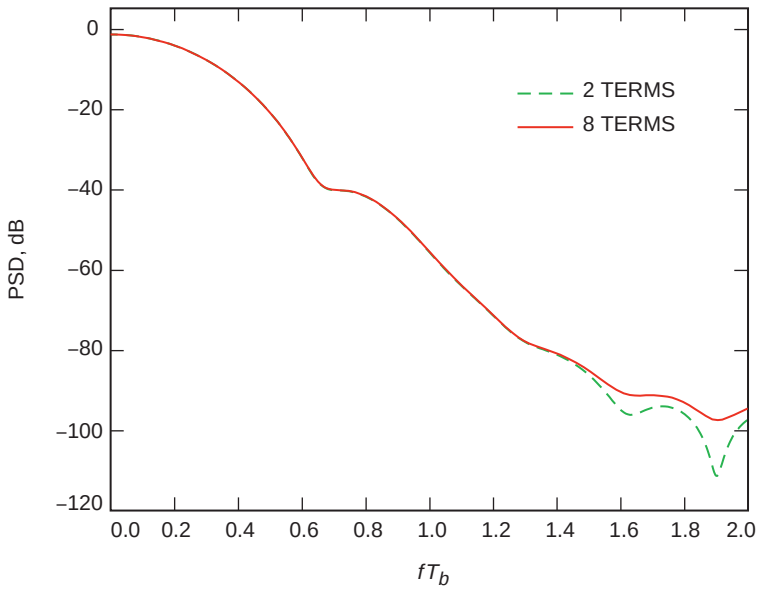

Fig. 4. A comparison of the complex baseband power spectral density of balanced GMSK for two and all eight AMP components.

similar behavior. To guarantee this assumption, we computed the autocorrelation and cross-correlation properties of the next (third) pulse sequence, $\{\tilde{a}_{2,n}\}$, as defined in the first equation of Eq. (44) as well as the corresponding terms that would contribute to the PSD. These results are given in the Appendix and will be used to identify the level above which the PSD computed from only the first two pulse streams is sufficient.

Illustrated in Figs. 5(a) and 5(b) is the complex baseband PSD of unbalanced GMSK [see Eqs. (34), (38), (41), and (42)] for $p = 0.45$ and $p = 0.20$ as well as computer simulation results based on a true GMSK signal. Here again we see that the dominant effect of the data unbalance occurs in the region of the main lobe. In the limit as $p \to 1$, the power spectrum would become a pair of delta functions at $f = \pm 1/4T_b$, each containing one half the total power. Using the results from the Appendix, the PSD of Fig. 5(b) was recomputed taking into account the addition of the third pulse stream. The comparison of these results is illustrated in Fig. 6. As previously anticipated, above a PSD level of -70 dB, the difference between the two results is undetected.

For the case of unbalanced precoded MSK, the PSD as computed from the superposition (sum) of Eqs. (49) and (50) is illustrated in Fig. 7(a) for $p = 0.55$ and in Fig. 7(b) for $p = 0.10$. Once again, results obtained from computer simulation are superimposed on these figures and indicate excellent agreement with the theory.

VII. Conclusion

The Laurent AMP representation of MSK-type modulations is particularly helpful in the evaluation of the power spectrum of such modulations in the presence of data imbalance. Specifically, the representation allows obtaining closed-form expressions for the power spectrum that clearly elucidate its partitioning into components due to the effective AMP pulse shapes and those due to the AMP sequence correlations. Furthermore, the nature of the PSD distortion produced by the imbalance, i.e., a tilt in the main lobe and a relative unbalance between the upper and lower side-lobe levels, is easily identifiable from the mathematical form of the results.

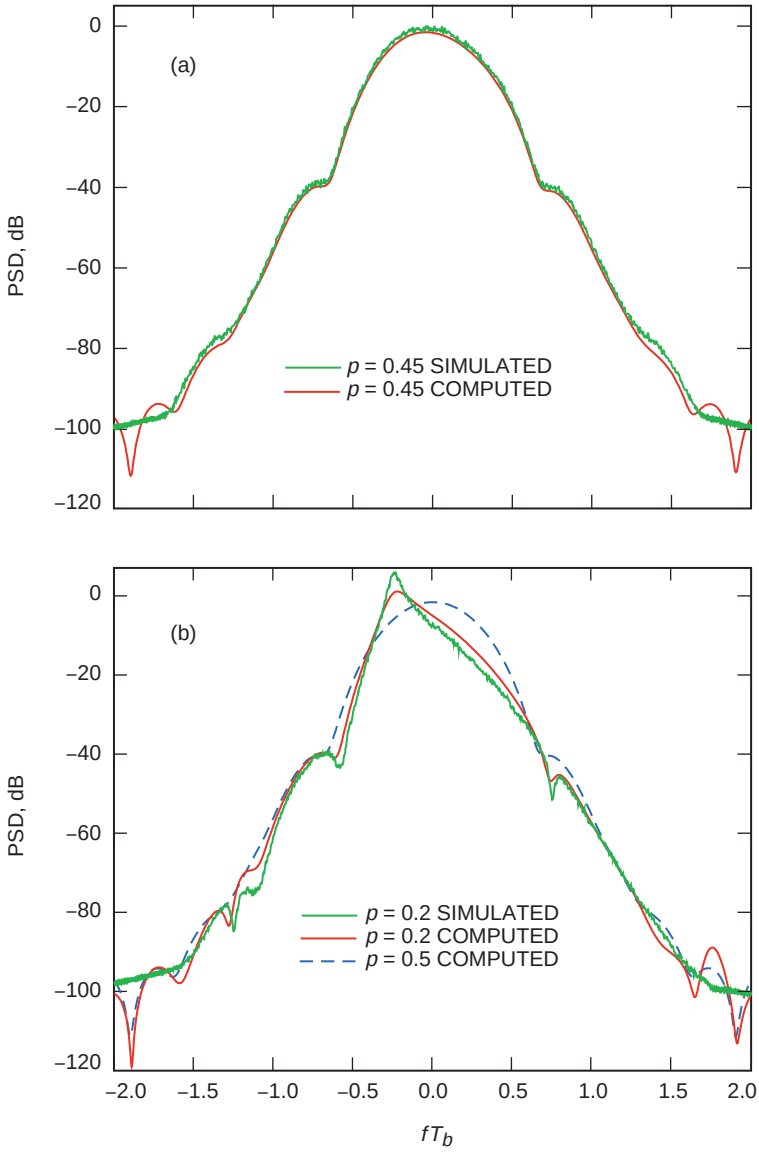

Fig. 5. The complex baseband power spectral density of unbalanced GMSK: (a) $p = 0.45$ and (b) $p = 0.2$.

References

[1] J. B. Anderson, T. Aulin, and C.-E. Sundberg, *Digital Phase Modulation*, New York and London: Plenum Press, 1986.

[2] J. Proakis, *Digital Communications*, New York: McGraw-Hill, 3rd ed., 1995.

[3] B. E. Rimoldi, "A Decomposition Approach to CPM," *IEEE Transactions on Information Theory*, vol. 34, no. 3, pp. 260–270, March 1988.

[4] P. A. Laurent, "Exact and Approximate Construction of Digital Phase Modulations by Superposition of Amplitude Modulated Pulses," IEEE Transactions on Communications, vol. COM-34, no. 2, pp. 150–160, February 1986.

[5] V. K. Prabhu and H. E. Rowe, "Spectra of Digital Phase Modulation by Matrix Methods," *Bell System Technical Journal*, vol. 53, no. 5, pp. 899–934, May–June 1974.

[6] V. K. Prabhu and H. E. Rowe, "Power Spectrum of a Digital, Frequency Modulation Signal," *Bell System Technical Journal*, vol. 54, no. 6, pp. 1095–1125, July–August 1975.

[7] M. K. Simon, S. M. Hinedi, and W. C. Lindsey, *Digital Communication Techniques: Signal Design and Detection*, Englewood Cliffs, New Jersey: PTR Prentice-Hall, 1995.

[8] U. Mengali and M. Morelli, "Decomposition of M-ary CPM Signals Into PAM Waveforms," *IEEE Transactions on Information Theory*, vol. 41, no. 5, pp. 1265–1275, September 1995.

[9] G. K. Kaleh, "Simple Coherent Receivers for Partial Response Continuous Phase Modulation," *IEEE Transactions on Selected Areas in Communications*, vol. 7, no. 9, pp. 1427–1436, December 1989.

[10] L. B. W. Jolley, *Summation of Series*, New York: Dover Publications, 1961.

[11] F. Amoroso, "Pulse and Spectrum Manipulation in the Minimum (Frequency Shift Keying (MSK) Format," *IEEE Transactions on Communications*, vol. COM-24, no. 3, pp. 381–384, March 1976.

[12] W. L. Martin, T.-Y. Yan, and L. Lam, *CCSDS-SFCG Efficient Modulation Methods Study: A Comparison of Modulation Schemes, Part 3: End-to-End System Performance*, SF17-28/D, SFCG Meeting, Galveston, Texas, September 16–25, 1997.

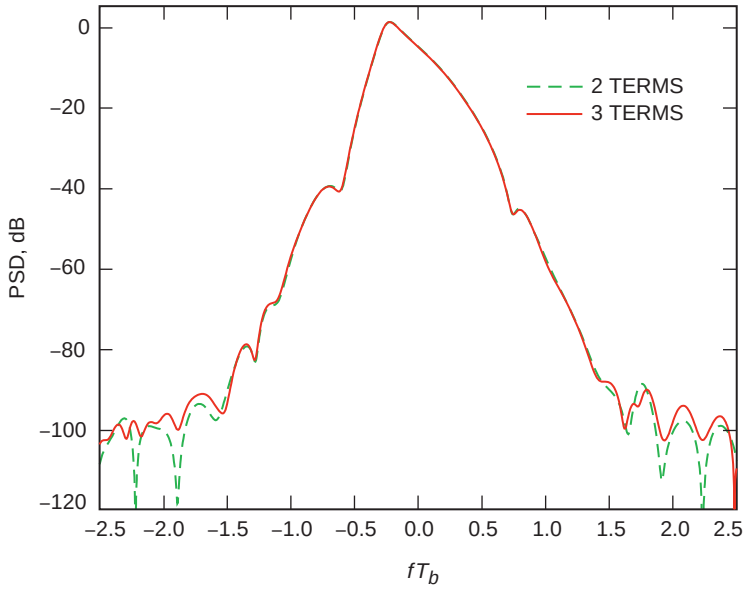

Fig. 6. A comparison of the complex baseband power spectral density of unbalanced GMSK for two and three AMP components, with $p = 0.2$.

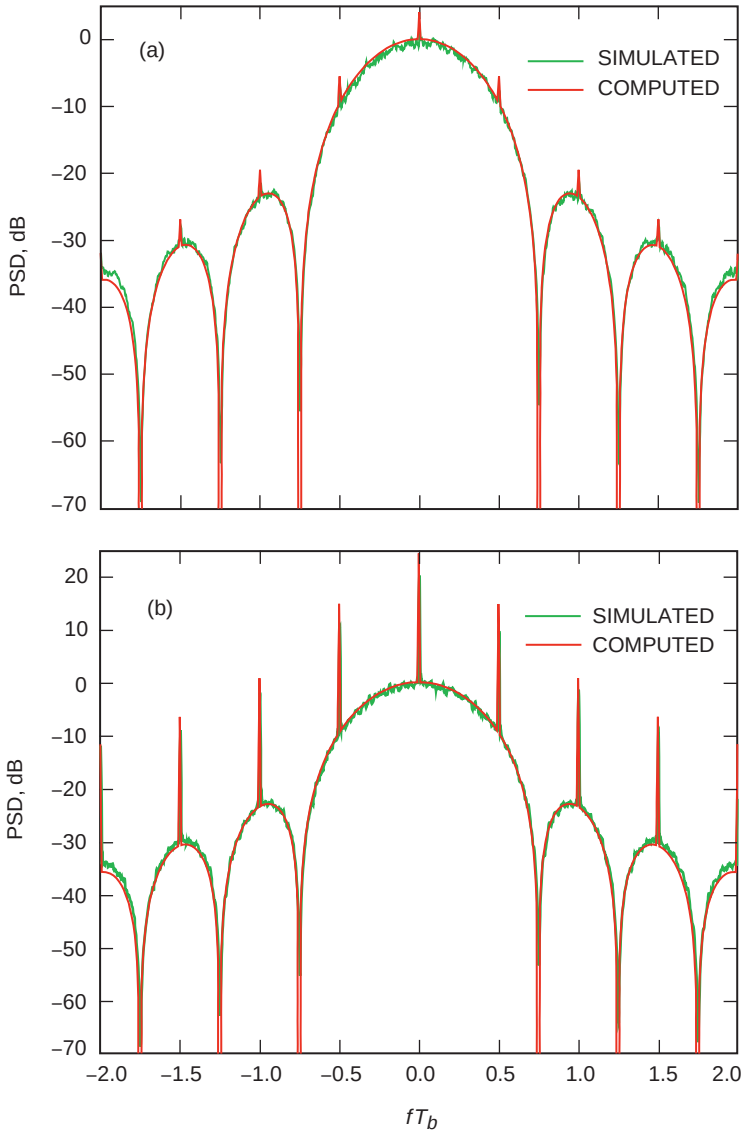

Fig. 7. The complex baseband power spectral density of unbalanced precoded MSK: (a) $p = 0.55$ and (b) $p = 0.1$.

Appendix

Correlation and Spectral Properties of the Third Pulse Stream in the AMP Representation of GMSK

From the defining recursion relation for the third pulse stream, $\{\tilde{a}_{2,n}\}$, as given in Eq. (42) together with the analogous relation for the first and second pulse streams, $\{\tilde{a}_{0,n}\}$ and $\{\tilde{a}_{1,n}\}$, as given in Eq. (15), it is straightforward to show that

$$R_{\tilde{a}_2}(l) \triangleq E\left\{\tilde{a}_{2,n}\tilde{a}^*_{2,n+l}\right\} = \begin{cases} 1, & l=0 \\ -j(1-2p)^3, & l=1 \\ -(1-2p)^4, & l=2 \\ [-j(1-2p)]^l, & l\geq 3 \end{cases}, \quad R_{\tilde{a}_1}(-l) = R^*_{\tilde{a}_1}(l) \tag{A-1}$$

and

$$R_{\tilde{a}_{20}}(l) \triangleq E\left\{\tilde{a}_{2,n}\tilde{a}^*_{0,n+l}\right\} = \begin{cases} [-j(1-2p)]^{l+1}, & l\geq 0 \\ (1-2p)^2, & l=-1 \\ j(1-2p)^2, & l=-2 \\ [j(1-2p)]^{-(l+1)}, & l\leq -3 \end{cases}, \quad R_{\tilde{a}_{02}}(-l) = R^*_{\tilde{a}_{20}}(l) \tag{A-2}$$

$$R_{\tilde{a}_{21}}(l) \triangleq E\left\{\tilde{a}_{2,n}\tilde{a}^*_{1,n+l}\right\} = \begin{cases} [-j(1-2p)]^l, & l\geq 2 \\ -j(1-2p)^3, & l=1 \\ (1-2p)^2, & l=0 \\ j(1-2p), & l=-1 \\ -(1-2p)^4, & l=-2 \\ [j(1-2p)]^{-l}, & l\leq -3 \end{cases}, \quad R_{\tilde{a}_{12}}(-l) = R^*_{\tilde{a}_{21}}(l) \tag{A-3}$$

The corresponding components needed to compute the PSD given in Section III are as follows:

$$S_{22}(f;p) = \frac{1}{T_b}|P_2(f)|^2 4p(1-p)\left[\frac{1}{2(1-2p)(1+\sin 2\pi f T_b)+4p^2}\right.$$

$$\left. +2(1-2p)\sin 2\pi f T_b + 2(1-2p)^2\cos 4\pi f T_b\right], \qquad P_2(f) \triangleq \mathcal{F}\{C_2(t)\} \tag{A-4}$$

$$S_{20}(f;p) = 8p(1-p)\ \mathrm{Re}\ \left\{ \left[\left(\frac{1}{2(1-2p)(1+\sin 2\pi f T_b) + 4p^2} - 1 \right) e^{j2\pi f T_b} \right.\right.$$

$$\left.\left. -j(1-2p)e^{j4\pi f T_b} \right] \frac{1}{T_b} P_0(f) P_2^*(f) \right\} \tag{A-5}$$

$$S_{21}\left(f;p\right) = 8p\left(1-p\right)\ \mathrm{Re}\ \left\{ \left[\left[j\left(1-2p\right) \right] e^{-j2\pi f T_b} + \frac{1}{2\left(1-2p\right)\left(1+\sin 2\pi f T_b\right) + 4p^2} - 1 \right.\right.$$

$$\left.\left. + \left(1-2p\right)^2 e^{j4\pi f T_b} \right] \frac{1}{T_b} P_1\left(f\right) P_2^*\left(f\right) \right\} \tag{A-6}$$